process of change in the ligation and to superposition of different sites.

The effect of various solvents on the morphology of ionomers is a subject of great interest and has been investigated in many systems, including Nafion and sulfonated polystyrene (SPS). In the latter system the effect of thermal treatment has been detected in SAXS studies; heating to 165 °C seems to induce the formation of the ionic peak that did not appear at ambient temperatures.[24] In an extended X-ray absorption fine structure (EXAFS) study of SPS neutralized by Mn^{2+} it was not possible, however, to detect changes in the local structure of the cation due to heat treatment.[25]

To the best of our knowledge this paper contains the first study that gives a detailed molecular picture of the solvation process. Most importantly, it is necessary to keep in mind that simply adding a solvent to a dry ionomer will in general not replace all the ligands with the most abundant solvent.

Conclusions

1. Cupric ions in dry Nafion soaked with CD_3CN are preferentially solvated by the water remaining in the membranes, even though the following ratios have been measured: $CD_3CN/Cu^{2+} = 118$, water/$Cu^{2+} = 2.5$.

2. In membranes soaked with CH_3CN the water ligands around the cation are partially replaced after one cycle of drying of the membranes. The isotope effect in acetonitrile seems to be due to a higher polarity of CD_3CN, compared to CH_3CN.

3. The details on the solvation process can be followed by an analysis of the superhyperfine (shf) structure from ^{14}N ligands. The major site detected after *two* cycles of drying of the membranes and soaking with CD_3CN or CH_3CN clearly indicated four nitrogen ligands in a tetrahedrally distorted tetragonal symmetry. The shf is seen on the $m_I = -^3/_2$ component of the parallel signal and on the perpendicular signal. The resolution of the shf pattern in the perpendicular orientation can be significantly improved by computer-calculated second-derivative presentation of ESR spectra.

4. Changes in the local environment of the cation at ambient temperature on a time scale of several weeks are detected from changes in the shf pattern and are thought to reflect a decrease in the tetrahedral distortion.

5. No evidence for clustering of cations is detected in fully neutralized membranes that underwent one cycle of drying and soaking with CH_3CN.

Acknowledgment. This research is supported by National Science Foundation Grant DMR-8718947 (ROW). The ESR spectrometer was purchased with NSF Grant DMR-8501312.

(24) Fitzgerald, J. J.; Kim, D.; Weiss, R. A. *J. Polym. Sci., Polym. Lett. Ed.* **1986**, *24*, 263.
(25) Register, R. A.; Sen, A.; Weiss, R. A.; Cooper, S. L. *Macromolecules* **1989**, *22*, 2224.

Homonuclear Three-Dimensional ^1H NMR Spectroscopy of Pike Parvalbumin. Comparison of Short- and Medium-Range NOEs from 2D and 3D NMR

André Padilla,[†] Geerten W. Vuister, Rolf Boelens, Gerard J. Kleywegt, Adrien Cavé,[†] Joseph Parello,[§] and Robert Kaptein*

Contribution from the Department of Chemistry, University of Utrecht, Padualaan 8, 3584 CH Utrecht, The Netherlands. *Received December 4, 1989*

Abstract: The short- and medium-range NOEs that can be obtained from 2D NOE spectra and homonuclear 3D HOHAHA-NOE spectra of the protein parvalbumin III of pike have been compared. An extensive analysis has been made of a 3D HOHAHA-NOE spectrum in ^1H_2O of the cross sections perpendicular to the ω_3 axis at the amide resonance frequencies, where most of the sequential connectivities can be found. A single 3D HOHAHA-NOE spectrum resulted in 455 3D cross peaks involving short- and medium-range NOEs on which the assignment of 108 amino acids residues could be based. The 3D data set allowed definition of the secondary structure better than was previously possible, by the observation of a series of new medium-range NOEs. In addition, the 3D spectrum indicated that the amino acid sequence of pike parvalbumin III contained an error and that the protein actually consists of 109 amino acid residues rather than 108 as previously thought.

Structure determination of proteins in solution by high-resolution NMR spectroscopy relies on nuclear Overhauser effects (NOEs), from which interproton distance constraints can be derived.[1] For proteins, the NOEs are generally obtained from 2D NOE spectra and can be observed for interproton distances less than about 5 Å. For such an analysis it is essential to obtain first the sequence specific assignments of the proton resonances. This assignment is usually carried out with a combination of two types of 2D spectra, one involving J coupling and the other NOE transfer. However, due to overlap in 2D spectra of proteins the analysis remains a laborious and sometimes impossible task.

The general idea behind the development of 3D NMR spectroscopy is to increase the resolution by correlating the resonance frequencies of three individual spins in three independent dimensions. In this respect, 3D experiments turn out to be very promising for the NMR study of macromolecules.[2,3] In the last few years, various homonuclear 3D experiments such as NOESY-COSY[4] and 3D NOE-HOHAHA (or NOESY-TOCSY)[5,6]

[†] Present address: Centre CNRS Inserm, Rue de la Cardonille, 34090 Montpellier, France.
[§] Present address: Unité Associée No. 1111, CNRS, Faculté de Pharmacie, 15 Avenue Charles Flahault, 34060 Montpellier Cédex, France.

(1) Wüthrich, K. *NMR of Proteins and Nucleic Acids*; Wiley: New York, 1986.
(2) Griesinger, C.; Sørensen, O. W.; Ernst, R. R. *J. Magn. Reson.* **1989**, *84*, 14-63.
(3) Boelens, R.; Vuister, G. W.; Padilla, A.; Kleywegt, G. J.; De Waard, P.; Koning, T. M. G.; Kaptein, R. In *Biological Structure, Dynamics, Interactions & Expression. Proceeding of the Sixth Conversation in Biomolecular Stereodynamics*; Sarma, R. H., Sarma, M. H., Eds.; Adenine Press: New York, 1989; in press.
(4) Griesinger, C.; Sørensen, O. W.; Ernst, R. R. *J. Magn. Reson.* **1987**, *73*, 574-579.
(5) Oschkinat, H.; Griesinger, C.; Kraulis, P. J.; Sørensen, O. W.; Ernst, R. R.; Gronenborn, A. M.; Clore, G. M. *Nature* **1988**, *332*, 374-376.

0002-7863/90/1512-5024$02.50/0

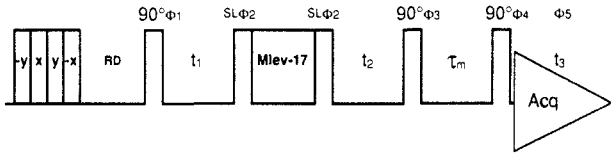

Figure 1. Pulse sequence for the 3D HOHAHA-NOE experiment. RD and τ_m correspond to the relaxation delay and the NOE mixing time, respectively. The phase cycling used is as follows: $\Phi_1 = y, -y, -x, x$; $\Phi_2 = -x, -x, -y, -y$; $\Phi_3 = y, y, -x, -x$; $\Phi_4 = y, y, x, x$; $\Phi_5 = y, -y, x, -x$.

have been developed. In these 3D spectra the chemical shift dispersion of the proton resonances is used to solve overlap problems in combination with magnetization transfer due to the NOE and J coupling. In addition, a 3D NOE-NOE experiment has recently been reported.[7] The 3D HOHAHA-NOE experiment[8,9] can be regarded as a combination of a 2D HOHAHA or TOCSY for the J interaction and a 2D NOE experiment. A particularly promising application is the assignment of ^1H spectra of proteins,[10] since it combines the magnetization transfers due to both NOE and J coupling in one single experiment.

It is also possible to use the chemical shift dispersion of the ^{15}N or ^{13}C to edit complex homonuclear 2D spectra. This is done, for instance, in HMQC-COSY and HMQC-NOESY[11] and the reverse NOESY-HMQC experiment.[12,13] The total number of cross peaks in such a heteronuclear 3D spectrum remains the same as in the corresponding homonuclear 2D spectrum, but the analysis is simplified by spreading the cross-peak information in the heteronuclear dimension. By contrast, in the homonuclear 3D spectrum the number of cross peaks may be larger, which allows a multiple checking of NOE interactions.

Here we report the assignment of sequential and medium-range 3D connectivities of the protein pike parvalbumin III. Pike parvalbumin III has previously been studied by 2D NMR, and the assignments of most of the proton resonances have been obtained.[14] The folding of the protein has been determined by distance geometry on the basis of the identified NOE distance constraints.[14] The solution structure of pike parvalbumin III shows a strong homology with the X-ray structures of the carp parvalbumin III[15] and pike parvalbumin II.[16] The general organization of the secondary-structure elements, as well as the packing of the hydrophobic residues, is well conserved. The major secondary-structure elements are six helices called A-F, which represent 50% of the total residues in the peptide regions 8-17, 26-32, 41-51, 60-64, 81-90, and 99-109, respectively. A short antiparallel β-sheet involves the two strands 57-59 and 96-98.

In the present paper, the sequential and medium-range NOEs extracted from a 3D HOHAHA-NOE spectrum are compared to those obtained from 2D NOE spectra. In this analysis, cross sections perpendicular to the ω_3 axis (ω_3 planes) are used, in particular at the amide resonance frequencies. The single-transfer NOE cross peaks present in the NOE plane of the 3D spectrum are analogous to those present in the 2D NOE spectrum and have not been included in this comparison. It will be demonstrated that a single 3D HOHAHA-NOE spectrum contains at least as much information necessary for the sequential analysis and the determination of secondary structure as a set of 2D NMR spectra. Moreover, the 3D spectrum showed that the primary structure of pike parvalbumin III was incorrect and that an extra alanine is present in the N-terminal part of the sequence.

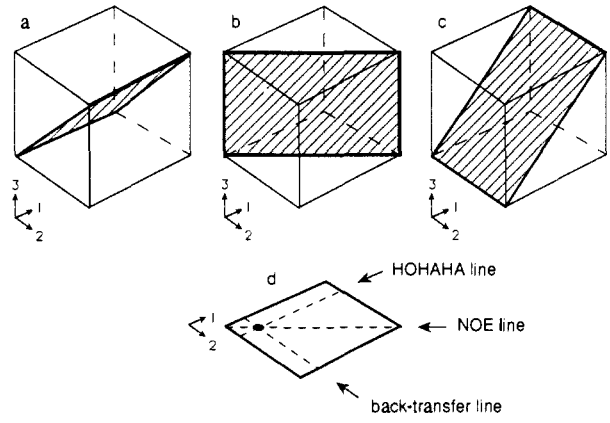

Figure 2. Schematic representation of cross-diagonal planes of a 3D HOHAHA-NOE spectrum: (a) HOHAHA plane ($\omega_2 = \omega_3$); (b) NOE plane ($\omega_1 = \omega_2$); (c) back-transfer plane ($\omega_1 = \omega_3$). A cross section perpendicular to the ω_3 direction, also called ω_3 cross section, (d) has three intersections with the HOHAHA, NOE, and back-transfer planes, labeled NOE, HOHAHA, and back-transfer lines (dotted lines), respectively.

Materials and Methods

The NMR sample was prepared as described previously.[14] The protein concentration was 7 mM in a mixture of 95% ^1H_2O and 5% ^2H_2O. The 3D experiment was recorded at 42 °C and pH 4.6.

The pulse sequence of the 3D HOHAHA-NOE experiment is shown in Figure 1. The HOHAHA and NOE mixing times were 44 and 150 ms, respectively. TPPI was applied for the t_1 time domain on the first 90° pulse and for the t_2 time domain on the last two 90° pulses and on the receiver phase. Axial peak suppression was carried out by phase cycling on the first pulse and on the receiver. Water suppression was done by presaturation during the relaxation delay of 0.6 s as well as during the NOE mixing time (τ_m) with the same radiofrequency source for the decoupler and the pulse transmitter. The HOHAHA mixing was obtained with an $(MLEV\text{-}17)_n$ pulse sequence of 38 ms, sandwiched between two 3-ms trim pulses.[17,18] All pulses were given with a 10-W continuous-wave amplifier ($\gamma B_1 = 10.7$ kHz). For each FID, four scans were taken without any dummy scans but with presaturation by four trim pulses of 1 ms each before the pulse sequence was started. The acquired data consisted of 246 t_1 × 256 t_2 × 512 t_3 data points. The HOHAHA-NOE spectrum was recorded on a Bruker AM 500 spectrometer, equipped with an Aspect 3000 computer. The total experiment time was 119 h of which 58 h was spent for disk transfers and reloading of the pulse programmer.

The processing was done on a μ VAX II computer with the TriTon software package written in Fortran77.[6] Sine-bell windows shifted by $\pi/3$ in t_3 and $\pi/2$ in t_2 and t_1 were used as apodization functions. The data were zero-filled once in the time domains t_1 and t_2 and Fourier transformed. The resulting spectrum contained 256 × 256 × 256 real spectral points. A third-order polynomial automatic base-line correction[19] was applied in each dimension.

For the analysis, all ω_3 cross sections at the amide resonance frequencies were plotted at identical contour levels, except for three planes that involved intense aromatic resonances.

Analysis of 3D HOHAHA-NOE Spectra. The general features of a 3D HOHAHA-NOE spectrum are presented in Figure 2. The two cross-diagonal planes, $\omega_2 = \omega_3$ and $\omega_1 = \omega_2$ (Figure 2a,b), contain information due to single HOHAHA or NOE transfers only and are therefore called the HOHAHA and NOE plane, respectively. The intersections of these two planes with an ω_3 cross section (Figure 2d) yield the lines with single transfers by HOHAHA or NOE, the so-called HOHAHA and NOE lines. All other cross peaks in the 3D spectrum correspond to double transfers. A special case is represented by the cross

(6) Vuister, G. W.; Boelens, R.; Kaptein, R. *J. Magn. Reson.* **1988**, *80*, 176-185.
(7) Boelens, R.; Vuister, G. W.; Koning, T. M. G.; Kaptein, R. *J. Am. Chem. Soc.* **1989**, *111*, 8525-8526.
(8) Oschkinat, H.; Cieslar, C.; Gronenborn, A. M.; Clore, G. M. *J. Magn. Reson.* **1989**, *81*, 212-216.
(9) Oschkinat, H.; Cieslar, C.; Holak, T. A.; Clore, G. M.; Gronenborn, A. M. *J. Magn. Reson.* **1989**, *83*, 450-472.
(10) Vuister, G. W.; Padilla, A.; Boelens, R.; Kleywegt, G. J.; Kaptein, R. *Biochemistry* **1990**, *29*, 1829-1839.
(11) Fesik, S. W.; Zuiderweg, E. R. P. *J. Magn. Reson.* **1988**, *78*, 588-593.
(12) Zuiderweg, R. P.; Fesik, W. *Biochemistry* **1989**, *28*, 2387-2391.
(13) Marion, D.; Kay, L. E.; Sparks, S. W.; Torchia, D. A.; Bax, A. *J. Am. Chem. Soc.* **1989**, *111*, 1515-1517.
(14) Padilla, A.; Cavé, A.; Parello, J. *J. Mol. Biol.* **1988**, *204*, 995-1017.
(15) Kretsinger, R. H.; Nockolds, C. E. *J. Biol. Chem.* **1973**, *248*, 3313-3326.
(16) Declercq, J.-P.; Tinant, B.; Parello, J.; Etienne, G.; Huber, R. *J. Mol. Biol.* **1988**, *202*, 349-353.
(17) Bax, A.; Davis, D. G. *J. Magn. Reson.* **1985**, *65*, 355-360.
(18) Davis, D. G.; Bax, A. *J. Am. Chem. Soc.* **1985**, *107*, 2820-2821.
(19) Boelens, R.; Scheek, R. M.; Dijkstra, K.; Kaptein, R. *J. Magn. Reson.* **1985**, *62*, 378-386.

Table I. Intensities of 3D Cross Peaks between $C^{\alpha}H$, $C^{\beta}H$, and NH Resonances of Residues in α Helices and β Sheets

connectivity		α-helix[a]		β-sheet[a]	
$d_{\alpha N}$	$C_{N\alpha N}(i,i,i+1)$	w	(8/48)	s	(4/4)
	$C_{\beta\alpha N}(i,i,i+1)$	wm	(37/48)	ws	(4/4)
d_{NN}	$C_{\alpha NN}(i,i,i+1)$	m	(26/48)	w	(1/4)
	$C_{\alpha NN}(i,i,i-1)$	m	(24/48)	w	(0/4)
	$C_{\beta NN}(i,i,i+1)$	wm	(14/48)	w	(0/4)
	$C_{\beta NN}(i,i,i-1)$	wm	(13/48)	w	(0/4)
$d_{\beta N}$	$C_{N\beta N}(i,i,i+1)$	wm	(4/48)	wm	(0/4)
	$C_{\alpha\beta N}(i,i,i+1)$	wm	(35/48)	wm	(1/4)
	$C_{\beta\beta' N}(i,i,i+1)$	v	(13/30)	v	(2/2)
$d_{\alpha N}(i,i+3)$	$C_{N\alpha N}(i,i,i+3)$	w	(3/36)		
	$C_{\beta\alpha N}(i,i,i+3)$	wm	(31/36)		

[a] The first column indicates the connectivities corresponding to single NOE transfer following the notation of Wüthrich.[1] The intensities of 3D cross peaks were calculated according to standard distances in an α helix and in a β sheet[1] and are classified as w (weak), m (medium), s (strong), and v (variable). The numbers in parentheses correspond to the number of connectivities observed via 3D cross peaks versus the number of connectivities expected on the basis of the secondary-structure elements present in pike parvalbumin. The $C^{\beta}H$ resonances for which chemical shift equivalence has been observed have not been included in the number of expected $C_{\beta\beta' N}(i,i,i+1)$ connectivities.

peaks observed on the back-transfer line (intersection with the back-transfer plane, $\omega_1 = \omega_3$), which correspond to double transfers with identical first and last spins.

The C notation used to label the 3D cross peaks in this paper is that introduced by Vuister et al.:[10]

$$C[x,y]_{abc}(i,j,k)$$

or simply

$$C_{abc}(i,j,k)$$

where $x,y \in \{NOE, J, ...\}$, $a, b, c \in \{N, \alpha, \beta, ...\}$, and i, j, k are residue numbers.

The x,y indication in square brackets refers to the first and second mixing processes in the 3D NMR experiment, respectively, i.e., NOE or J coupling (for HOHAHA, COSY, etc.). The spins involved (a, b, c of the residues i, j, k) are denoted by N for NH, α for $C^{\alpha}H$, β for $C^{\beta}H$, etc. Throughout this paper an abbreviated notation will be used by omitting the indices $[x,y]$, which are by default [J,NOE] for the 3D HOHAHA-NOE spectrum. Thus, $C_{abc}(i,j,k)$ will be equivalent to $C[J,NOE]_{abc}(i,j,k)$.

The 3D connectivities involving $C^{\alpha}H$, $C^{\beta}H$, and NH protons expected in ω_3 cross sections at the amide resonance frequencies are listed in Table I. The theoretical intensities of the 3D cross peaks are calculated on the basis of a two-spin approximation for the NOE transfer and the HOHAHA transfer.[10] The strongest cross peak expected is the $C_{N\alpha N}(i,i,i+1)$ in a β sheet. This is due to the large $^3J_{\alpha N}$ coupling constant and the short $d_{\alpha N}$ distance in β sheets. The intensities of the 3D cross peaks involving $C^{\beta}H$ protons are difficult to define since the variation in the dihedral angle χ_1 will affect both the NOE intensity and the $^3J_{\alpha\beta}$ coupling.

Results and Discussion

For the analysis of a 3D HOHAHA-NOE spectrum it is convenient to use ω_1, ω_2, or ω_3 planes or any combination of them. Here we have chosen to use ω_3 planes at the amide frequencies for the following reasons: First, the intensity of the noise that is observed in planes perpendicular to the acquisition domain (t_1/t_2 noise) is lower in the ω_3 planes of NH protons than in other ω_3 planes. This noise is caused by instrumental instabilities and is more intense in the ω_3 planes of the sharp and intense resonances such as the aromatic and aliphatic proton resonances, than in ω_3 planes of the broader NH protons. Second, most of the sequential and medium-range contacts can be observed in the ω_3 NH planes (cf. Table I). We will show how these connectivities can be found in these planes and compare the short- and medium-range NOEs present in the 2D and 3D spectra of pike parvalbumin.

The assignments of the 3D cross peaks were made by comparison with those obtained previously from the analysis of a series of 2D spectra, i.e. COSY, relayed coherence transfer COSY, 2D HOHAHA, and 2D NOE, of pike parvalbumin III at 360, 500, and 600 MHz, at pH 6.1, 4.4, and 4.8 and at 62, 52, and 42 °C. However, even with this extensive set of 2D spectra, some cross peaks could not be assigned due to overlap. As an example, in the region 1.4–1.6 ppm/4.1–4.2 ppm, the $C^{\alpha}H$–$C^{\beta}H_3$ correlations of four alanines are present. Neither the analysis of the antiphase patterns expected in the COSY for these AX_3 spin systems nor the relayed NH–$C^{\beta}H_3$ connectivities in 2D HOHAHA or RCT-COSY experiments allowed unambiguous assignments. A similar situation exists in the region where the $C^{\gamma}H$–$C^{\delta}H$ correlations of lysines are located.

The 3D cross peaks that remained unassigned after this first comparison between the 2D data set and the 3D spectrum were assigned in the following way. Every pattern of 3D cross peaks parallel to the HOHAHA line in an ω_3 cross section is potentially a spin system or part of a spin system. A search over the ω_3 NH cross sections was carried out with the aim to observe the same pattern in other ω_3 cross sections. If the same set of 3D cross peaks had been assigned in an earlier stage, then the corresponding pattern can be identified. For long side-chain residues the assignment can be difficult, since the HOHAHA transfer in such cases gives an extensive set of possibly incomplete correlattions. However, in the simpler cases such as for alanine spin systems this could be done as will be discussed below.

Spin System Assignments and Correction of the Amino Acid Sequence. The primary structure of pike parvalbumin has been previously established by enzymatic and chemical cleavage and Edman degradation.[20,21] It was found that pike parvalbumin III has a high homology of about 60% with other parvalbumins. However, a significant difference was the absence of residue number 2. This primary sequence has been used previously to obtain the ^1H assignments by 2D NMR at 360 MHz of the pike parvalbumin III.[14] Seventeen alanines could be assigned sequentially. One remaining alanine spin system could not be assigned and was therefore assumed to correspond to the unassigned Ala 40. However, no sequential NOEs were observed between Ser 39, Ala 40, and Asn 41. Sequential connectivities found in more recent 500-MHz NOE spectra of parvalbumin indicated that Ala "40" was misassigned and in fact could correspond to an N-terminal alanine.

At that stage, the assignment of the spin system of Ala 40 was still lacking due to overlap in the 2D spectra. The 3D HOHAHA-NOE spectrum allowed us to solve this problem. In the ω_3 NH cross section of Asn 41 (Figure 3b) intraresidue cross peaks are observed that interconnect the NH, $C^{\alpha}H$, and $C^{\beta}H$ resonances of Asn 41. The unlabeled 3D cross peaks in Figure 3b are connectivities involving the NH or Thr 82. The remaining cross peaks, labeled $C_{\alpha\beta N}(40,40,41)$ and $C_{\beta\alpha N}(40,40,41)$, provide the connection to the spin system of Ala 40. The ω_3 NH cross section of this residue is shown in Figure 3a, with the intraresidue connectivities indicated. The AX_3 part of the spin system of Ala 40 is also observed in the ω_3 NH plane of Val 43 via the $C_{\beta\alpha N}(40,40,43)$ medium-range connectivity (Figure 3c). By 2D NMR this assignment was not possible due to the overlap of the $C^{\alpha}H$–$C^{\beta}H_3$ cross peaks of Ala 40, Ala 31, Ala 80, and Ala 88 in the region 1.4–1.6 ppm/4.1–4.2 ppm. Thus, all alanine cross peaks have now been accounted for, and the primary sequence has to be modified to accommodate an extra alanine in position 2. Subsequently, the presence of one extra alanine was confirmed by mass spectroscopy (Adrien Cavé, personal communication). The sequence now starts as Ala 1-Ala 2-Lys 3-etc., which makes it more homologous with the other parvalbumins.

Another example where the 3D spectrum helps to resolve overlap is in the identification of long side-chain resonances. For instance, in the 3D spectrum the correlations between $C^{\beta}H$ and $C^{\gamma}H$ of lysines can be relayed to the amide proton, thus giving a better resolution. In this way assignments for lysines could be made in those cases where the chemical shift difference of $C^{\beta}H$ and $C^{\gamma}H$ resonances was greater than the digital resolution (i.e., 25 Hz/point). For instance, in the case of Lys 44 (Figure 3d) on the line of the $C^{\epsilon}H$ resonances two cross peaks could be

(20) Frankenne, F.; Joassin, L.; Gerday, Ch. *FEBS Lett.* **1973**, *35*, 145–147.

(21) Gerday, C. *Eur. J. Biochem.* **1976**, *70*, 305–318.

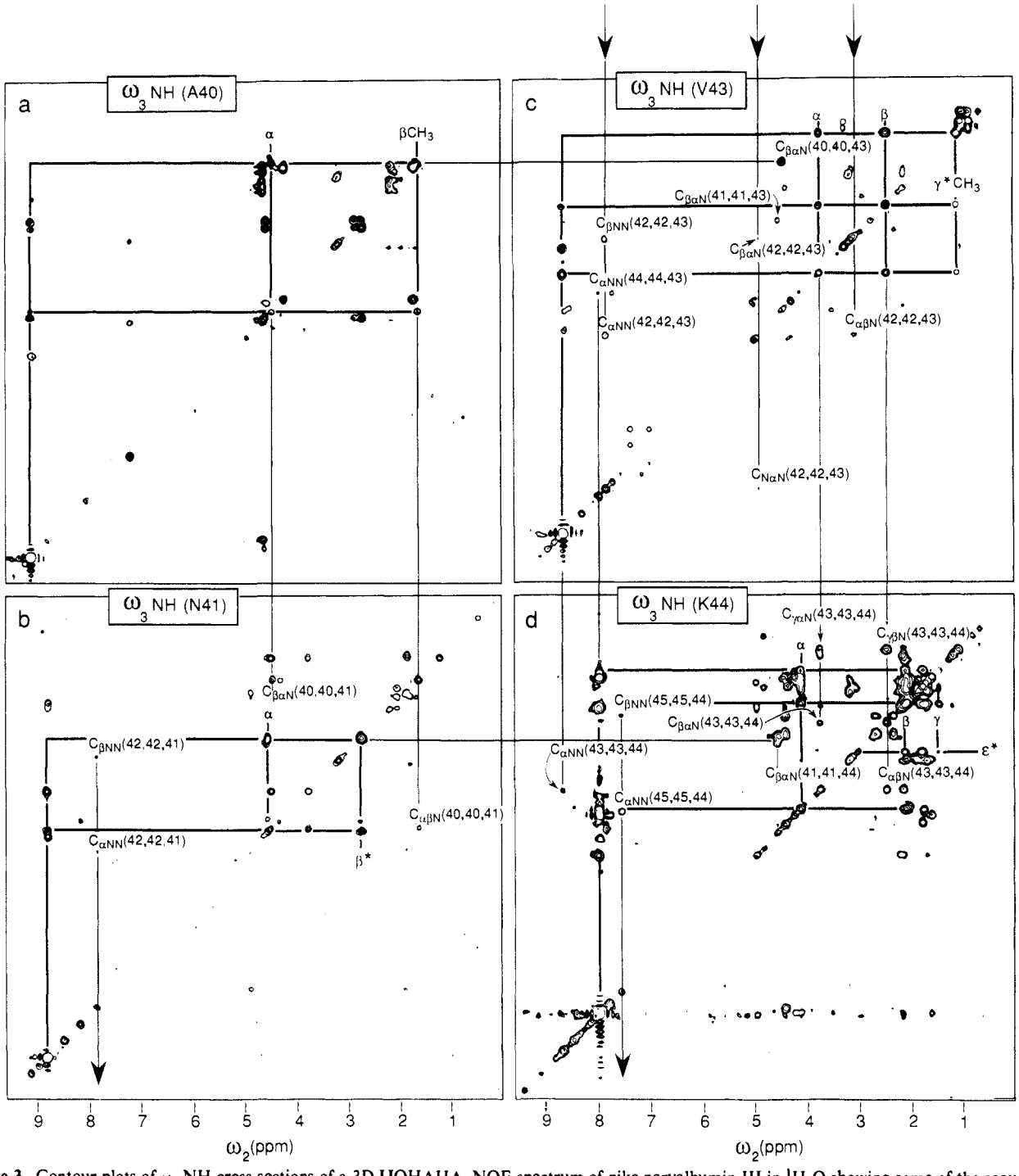

Figure 3. Contour plots of ω_3 NH cross sections of a 3D HOHAHA–NOE spectrum of pike parvalbumin III in ^1H_2O showing some of the sequential connectivities for the peptide fragment Ala 40–Lys 45. The 3D cross peaks involving sequential, $d_{\alpha N}$, d_{NN}, and $d_{\beta N}$, and medium-range, $d_{\alpha N}(i,i+3)$, NOE connectivities are labeled according to the notation introduced by Vuister et al.[10] The intraresidue 3D cross peaks are indicated by the letters α, β, γ, and δ at lines corresponding with the $C^\alpha H$, $C^\beta H$, $C^\gamma H$, and $C^\delta H$ proton resonances, respectively. In the cases of methyl groups of valines and methylene groups, chemical shift equivalences are denoted by asterisks. Bold lines are used to outline 3D intraresidue connectivities. Vertical lines and horizontal thin lines are used to indicate the sequential connectivities and $d_{\alpha N}(i,i+3)$ 3D connectivities, respectively.

identified as $C_{\epsilon\gamma N}(44,44,44)$ and $C_{\epsilon\beta N}(44,44,44)$ and are indicated by the labels β and γ for one $C^\beta H$ and one $C^\gamma H$ resonance, respectively. The remaining $C^\beta H$ and $C^\gamma H$ both contribute to the third strong 3D cross peak, which lies on the ϵ^* line between the β and γ lines.

3D Sequential Assignments. Recently, we showed how 3D NOE–HOHAHA and 3D HOHAHA–NOE spectra could be used for sequential assignments of proteins.[10] The method relies on the possibility for multiple checking of each sequential $d_{\alpha N}$, $d_{\beta N}$, or d_{NN} connectivity in various cross sections of the 3D spectrum. This is illustrated in Figure 3, in which a minimum set of ω_3 cross sections have been selected for the stretch Ala 40 up to Lys 45. A more extensive set of figures is available as supplementary material where the assignment of the complete helix C of parvalbumin is shown. The sequential connectivities between Ala 40 and Asn 41 have been discussed above. Continuing to Asp 42, the $C_{\alpha NN}(42,42,41)$ and $C_{\beta NN}(42,42,41)$ can be found in Figure 3b, both involving the $d_{NN}(42,41)$ connectivity. The spin system of Asp 42 can also be identified in the ω_3 NH cross section of Val 43 by the $C_{\beta NN}(42,42,43)$, $C_{\alpha NN}(42,42,43)$, $C_{\beta\alpha N}(42,42,43)$, $C_{N\alpha N}(42,42,43)$, and the $C_{\alpha\beta N}(42,42,43)$ connectivities, as can be seen in Figure 3c. In a similar way, a subset of the Val 43 spin system is observed in the ω_3 NH cross section of Lys 44 (Figure 3d) by the $C_{\alpha NN}(43,43,44)$, $C_{\gamma\alpha N}(43,43,44)$, $C_{\gamma\beta N}(43,43,44)$, and the $C_{\alpha\beta N}(43,43,44)$ connectivities. This is also indicated by the vertical lines starting from the NH, $C^\alpha H$, and

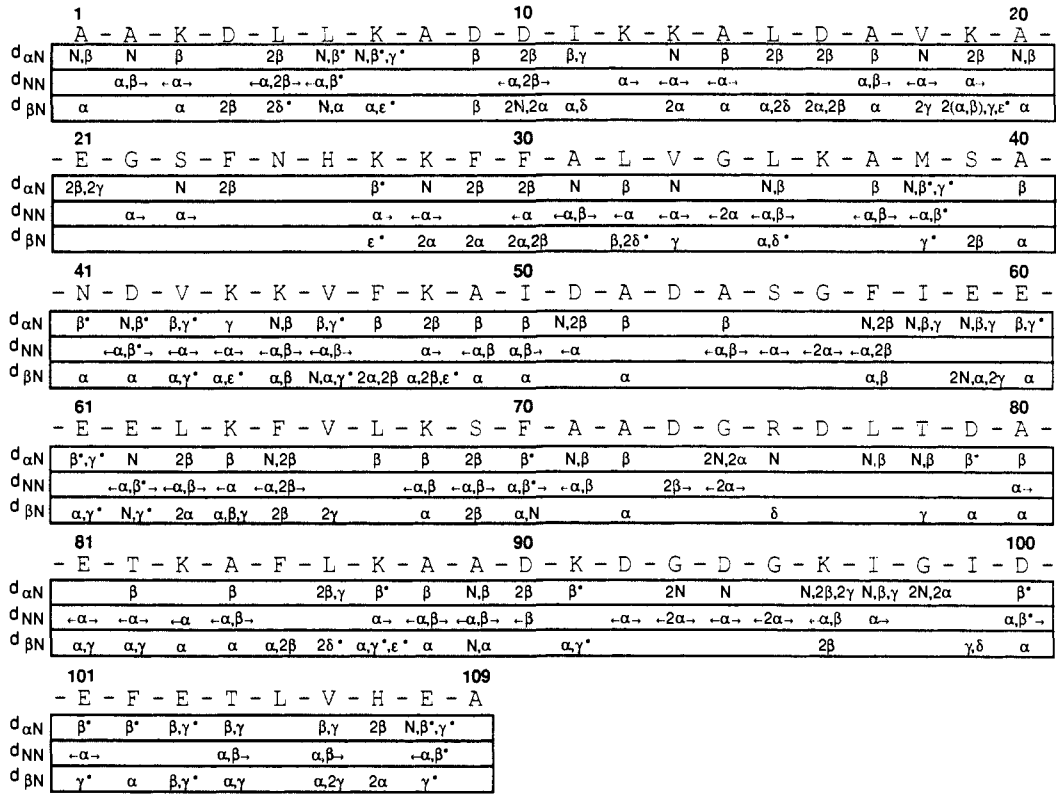

Figure 4. Sequence-specific assignments for 3D cross peaks of the ^1H 3D HOHAHA–NOE spectrum of pike parvalbumin III in ^1H_2O. The individual entries $d_{\alpha N}$, d_{NN}, and $d_{\beta N}$ correspond to short-range NOEs. The resonances involved in the HOHAHA transfers are labeled with greek letters with the same conventions as used in Figure 3. In cases of nonequivalence of $C^{\alpha}H$ resonances of glycines and $C^{\beta}H$ resonances of methylene groups, the number in front corresponds to the number of observations. In the case of 3D cross peaks of the d_{NN} type, the left and right arrows indicate $d_{NN}(i,i-1)$ and $d_{NN}(i,i+1)$ NOEs, respectively.

$C^{\beta}H$ resonances of Val 43 in Figure 3c connecting it with Figure 3d. The $C_{\beta NN}(45,45,44)$ and $C_{\alpha NN}(45,45,44)$ cross peaks establish the next sequential link from Lys 44 to Lys 45.

Figure 4 summarizes the 3D sequential connectivities that have been identified. It is clear that the information is highly redundant. For instance, it can be seen that the $d_{\alpha N}$ and the $d_{\beta N}$ occur many times, up to six times for the $d_{\beta N}$ between residues 19 and 20. This improves the reliability of the assignments, since the sequential NOEs can now be picked up on several resonance positions. This is very useful for large molecules where the overlap problem is considerable.

In Figure 5, the sequential NOEs found via the 3D connectivities are compared with those extracted from the set of 2D NOE spectra. In general, it can be seen that there is a large correspondence in the information between the 2D and 3D data sets. From the 3D spectrum, 67 d_{NN}, 86 $d_{\alpha N}$, and 75 $d_{\beta N}$ connectivities could be identified. From the 2D spectra these numbers were 83, 84, and 74, respectively. Some connectivities are missing in the 2D spectra due to overlap situations. For His 26 the NH is absent probably because of exchange broadening. On the other hand, some connectivities that were clearly observed in the 2D spectra are absent in the 3D spectrum. Partly, this is due to the unfavorable transfer efficiency that occurs as a result of the double transfer. Secondly, the fact that for the 3D experiment a pulse sequence of longer duration is used makes this experiment more sensitive to relaxation effects. This latter effect is of particular importance for the sequential connectivities involving two amide protons because of the relatively short T_2 relaxation times of these protons. Another problem is the lower digital resolution per domain for this 3D data set, which increases the number of cases of chemical shift coincidence.

NOEs corresponding to d_{NN} are widely seen in α-helical structures and lead to cross peaks of weak or medium intensity in the 3D HOHAHA–NOE spectrum (cf. Table I). On the basis of the positions of the six helices of pike parvalbumin III, as determined by 2D NMR, 48 of these d_{NN} connectivities are expected. Of these, 15 are lacking in the 3D spectra (Figures 4 and 5). Overlap of the amide resonances in the 3D spectrum (at the digital resolution of 25 Hz/point) for pairs of neighboring residues accounts for five of the missing d_{NN} connectivities (i.e., Ala 8-Asp 9, Ile 11-Lys 12, Ala 49-Ile 50, Leu 105-Val 106, and Glu 108-Ala 109). Another overlap situation occurs for the amide protons of Ala 14 and Asp 16, so that the d_{NN} connectivities with the NH of Leu 15 occur in the same ω_3 NH cross section. A strong 3D cross peak involves either $C_{\alpha NN}(15,15,14)$ or $C_{\alpha NN}(15,15,16)$ or both, but cannot be assigned to any of the individual connectivities. Some of the other missing cross peaks could be due to low transfer efficiencies in either the HOHANA or NOE transfer steps. For example, this can be the case for Leu 86 and Phe 102 since they have weak $C^{\alpha}H$–NH HOHAHA cross peaks both in the HOHAHA plane of the 3D spectrum and in the 2D HOHAHA spectrum. It should be noted that 43 of these 48 potential d_{NN} connectivities were found in the 2D spectra.

Altogether, in the 3D HOHAHA–NOE spectrum of parvalbumin, 152 3D cross peaks involving $d_{\alpha N}$ NOEs, 157 involving d_{NN} NOEs, and 145 involving $d_{\beta N}$ NOEs were found (cf. Figure 4). Additional information for sequential assignments can in principle be found in the ω_3 cross sections of $C^{\alpha}H$ and $C^{\beta}H$ resonances through the $C_{\alpha N\alpha}(i,i,i-1)$, and $C_{\alpha N\beta}(i,i,i-1)$ connectivities, respectively. However, due to a higher noise level in these planes, which are close to the water resonance, they have not been used systematically. Some ω_3 $C^{\alpha}H$ cross sections have been examined in order to identify missing sequential contacts. For instance, the $C_{\alpha N\alpha}(106,106,105)$ connectivity in the ω_3 $C^{\alpha}H$ cross section of Leu 105 allowed the identification of a sequential step between Leu 105 and Val 106.

3D Correlations Involving Medium-Range NOEs. Identification of medium-range connectivities is essential for the determination of the secondary-structure elements in a protein. Most of the 3D connectivities that identify the $d_{\alpha N}(i,i+2)$ and $d_{\alpha N}(i,i+3)$ medium-range NOEs are of the type $C_{\beta\alpha N}(i,i,i+2)$ and $C_{\beta\alpha N}(i,i,i+3)$. This is due to the efficient HOHAHA transfer between the $C^{\alpha}H$ and $C^{\beta}H$ protons in these connectivities. In addition, NH and $C^{\gamma}H$ resonances are found to be involved in some of the 3D

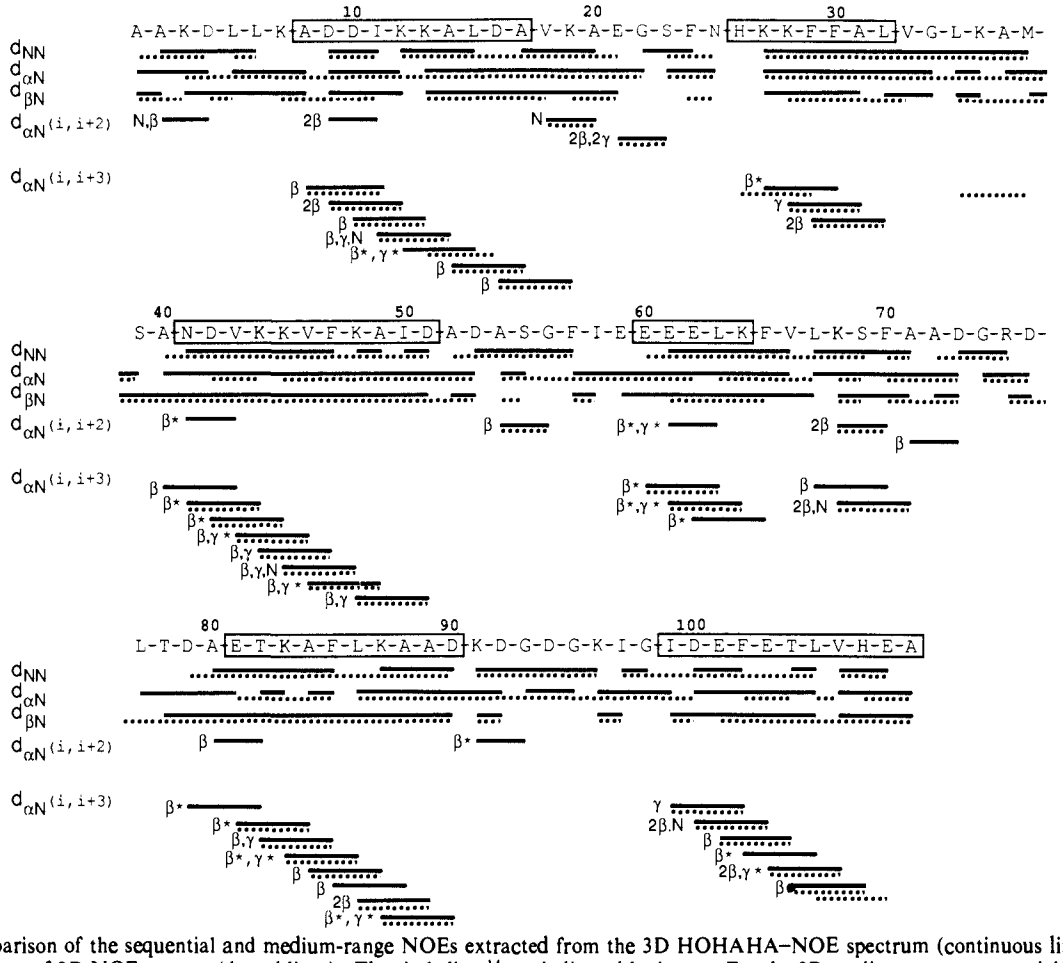

Figure 5. Comparison of the sequential and medium-range NOEs extracted from the 3D HOHAHA–NOE spectrum (continuous lines) and those obtained from a set of 2D NOE spectra (dotted lines). The six helices[14] are indicated by boxes. For the 3D medium-range connectivities, the NOEs are labeled $d_{\alpha N}(i,i+2)$ and $d_{\alpha N}(i,i+3)$. The HOHAHA pathways are labeled with the same conventions as used in Figure 4.

medium-range $i,i+2$ and $i,i+3$ connectivities (cf. Figure 5).

Examples of $C_{\beta\alpha N}(i,i,i+3)$ connectivities are illustrated in Figure 3 by the $C_{\beta\alpha N}(40,40,43)$ and the $C_{\beta\alpha N}(41,41,44)$ cross peaks. The occurrence of these connectivities suggests that the starting residue of helix C is Ala 40 instead of Asn 41. Due to the structural symmetry of the CD and EF domains of parvalbumin, homologous sets of NOEs are found for the residues in these two regions. The $C_{\beta\alpha N}(79,79,82)$ and $C_{\beta\alpha N}(81,81,84)$ medium-range connectivities present for the N-terminal part of helix E would suggest that this helix could extend to Asp 79, making it more similar to helix C. Most of the other $d_{\alpha N}(i,i+3)$ medium-range connectivities derived from the analysis of the 3D spectrum are in good agreement with those observed in the 2D NOE spectra. However, three medium-range connectivities that were seen in 2D spectra, i.e., $d_{\alpha N}(13,16)$, $d_{\alpha N}(35,38)$, and $d_{\alpha N}(105,108)$, could not be observed in the 3D spectrum because of overlap due to the lower digital resolution. No 3D cross peaks were observed for the $d_{\alpha N}(26,29)$, $d_{\alpha N}(47,50)$, and $d_{\alpha N}(106,109)$ based connectivities. The weak $^3J_{\alpha\beta}$ coupling constants observed for His 26 can explain the loss of the 3D $C_{\beta\alpha N}(26,26,29)$ cross peaks. The $d_{\alpha N}(47,50)$ and $d_{\alpha N}(106,109)$ NOEs were not observed in 2D spectra either. It can be seen from Figure 5 that the set of $d_{\alpha N}(i,i+3)$ connectivities obtained from the analysis of the 3D spectrum is slightly larger (37) than the set obtained from the analysis of 2D spectra (33). Several $d_{\alpha N}(i,i+3)$ could not be assigned in the 2D spectra due to overlap, i.e., $d_{\alpha N}(12,15)$, $d_{\alpha N}(27,30)$, $d_{\alpha N}(40,43)$, $d_{\alpha N}(62,65)$, $d_{\alpha N}(67,70)$, $d_{\alpha N}(79,82)$, $d_{\alpha N}(85,88)$, and $d_{\alpha N}(102,105)$. In the 3D they have been observed by the relay to side-chain resonances.

Loop regions and turns give rise to a small number of medium-range connectivities. Four $d_{\alpha N}(i,i+2)$ NOEs had been identified on the basis of the 2D NMR data sets (cf. Figure 5). Seven new $d_{\alpha N}(i,i+2)$ connectivities have been found in the 3D HOHAHA–NOE spectrum. Of these, four are located at the beginning of helices A, C, D, and E.

Table I shows the ratios of the observed number of 3D cross peaks in the 3D HOHAHA–NOE spectrum of parvalbumin versus the number of expected 3D cross peaks. For α helices, the highest ratios are observed for the sequential $C_{\beta\alpha N}(i,i,i+1)$, $C_{\alpha NN}(i,i,i\pm1)$, and the $C_{\alpha\beta N}(i,i,i+1)$. We also note that the medium-range $C_{\beta\alpha N}(i,i,i+3)$ have a high score. This is probably related to the fact that in α helices the favored χ_1 values are such that there is usually one $C^\beta H$ proton with a large $^3J_{\alpha\beta}$ coupling. The steric restrictions do not apply to residues at the beginning of an α helix. In this case, the situation of two small $^3J_{\alpha\beta}$ couplings is possible. This may be the reason for the absence of the $C_{\beta\alpha N}(26,26,29)$ cross peaks. The low occurrence of $C_{N\alpha N}$ and $C_{N\beta N}$ can be explained by the relatively small $^3J_{\alpha N}$ in α helices in combination with the larger line width for the amide protons giving weak HOHAHA transfer. For β-sheet structures the ratios of Table I are less statistically relevant since only four sequential connectivities are expected in parvalbumin. Nevertheless, all the expected $C_{N\alpha N}(i,i,i+1)$ and $C_{\beta\alpha N}(i,i,i+1)$ 3D cross peaks have been observed.

Conclusions

Comparison with the data available from a set of 2D spectra shows that the information contained in a limited part of the 3D HOHAHA–NOE spectrum is quite extensive. One single 3D HOHAHA–NOE spectrum of parvalbumin allowed the observation of 455 3D cross peaks involving short- and medium-range NOEs on which the sequential assignment of 108 amino acid residues could be based. Because of the large number of 3D cross peaks, the sequential analysis becomes more reliable. The 3D HOHAHA–NOE spectrum of parvalbumin also allowed the correct assignment of all alanine residues including the formerly misassigned Ala 40 and the new Ala 2. In addition, new assignments of lysine side-chain protons could be made. Another advantage of a single 3D spectrum versus a set of 2D spectra is that conformational changes due to pH and temperature variations

are avoided. One 3D spectrum in principle contains all the information needed for the assignments and the secondary-structure analysis. The real measuring time that corresponds to both the pulse sequence duration and the data acquisition time was 61 h for this 3D HOHAHA–NOE experiment, since effects of relaxation during data-transfer operations were suppressed by presaturation trim pulses. This is comparable to the time needed to obtain a set of good 2D NOE and 2D HOHAHA spectra.

Despite the low efficiency due to the double transfer in a 3D experiment, the resulting sensitivity is still remarkably good. The intensities of the 3D cross peaks involving a d_{NN} transfer are strongly affected by the short T_1 and T_2 relaxation times of the NH protons. In order to obtain optimum sensitivity, both the values of the NOE and HOHAHA mixing times and the choice for the maximum length of the t_1 and t_2 evolution periods have to be adjusted. The replacement of the MLEV-17 by a "clean" pulse sequence that compensates for ROESY effects will be another improvement.[22] Such optimizations should be important for 2D spectroscopy as well but are essential in 3D in order to be able to observe 3D cross peaks of low intensity.

We found in the 3D spectrum new medium-range connectivities that better define the secondary-structure elements than was possible with the 2D NOE spectra. An extension of the analysis of the 3D HOHAHA–NOE spectrum to cross sections other than those at the amide frequencies will yield additional long-range NOEs that are essential for determining the overall folding. Some of these long-range contacts were already identified in the symmetry-related 3D NOE–HOHAHA spectrum of parvalbumin.[10]

It should be realized that the present work did not entail an ab initio assignment of parvalbumin from a 3D HOHAHA–NOE spectrum but that it still referred to the assignments as they were obtained previously from 2D spectra. However, our results suggest that a 3D assignment should be possible, since all ingredients that were present in the 2D set and used in the previous assignment work could also be identified in the 3D spectrum. In fact, the information contained in the 3D spectrum was highly redundant in characterizing spin systems. For many proteins and some biomolecules with a limited chemical shift dispersion, such as oligosaccharides, the overlap of resonances is the major bottleneck both in the assignment procedure and in the characterization of the NOE cross peaks used for the 3D structure analysis. In this case, the redundancy of information becomes very useful, since it offers the possibility to check proposed assignments in a systematic way on different cross sections. A practical problem in the analysis is related to the size of the 3D data set. In the 3D HOHANA–NOE spectrum of parvalbumin, more than 10 000 cross peaks are present. Recently, computer programs have been developed for both bookkeeping and assignment purposes.[23-26] Such automation should be very helpful in the analysis of 3D data sets, which are an ideal input for such programs.

One might ask what size of proteins can be studied by 3D HOHAHA–NOE. Parvalbumin contains 109 amino acids and gives both excellent 2D NOE and 2D HOHAHA spectra. The high quality of the 3D spectra is therefore not surprising. However, for molecules larger than about 15 kD, two problems arise: first, the increase in the number of resonances and, second, the increae of line width, which both lead to overlap of resonances. The first problem can be resolved by the application of 3D methods, but the second leads to a decrease of HOHAHA transfer efficiency that will reduce the cross-peak intensity in the 3D HOHAHA–NOE spectra. In this respect, it has been shown that heteronuclear 3D HMQC–NOESY can be applied for larger molecules due to the large ^{15}N–^{1}H coupling. Nevertheless, the assignment of spin systems, which is part of the conventional sequential assignment procedure, still relies on J interactions. Therefore, it is more likely that assignment strategies, which are less dependent on J coupling information, such as the main-chain-directed strategy,[27] will become essential for describing the NMR spectra of large proteins, which benefit from both heteronuclear and homonuclear 3D NMR.

Acknowledgment. We thank Dr. Gérard Etienne for the purification of the pike parvalbumin III. This work was supported by The Netherlands Foundation for Chemical Research (SON) with financial aid from the Nederlands Organization for the Advancement of Research (NWO) and by a research grant from the European Community (ST2J-0291).

Supplementary Material Available: Two figures giving the assignments of the ω_3 NH cross sections for the peptide fragment Ala 40–Asp 51 (2 pages). Ordering information is given on any current masthead page.

(22) Griesinger, C.; Ernst, R. R. *J. Am. Chem. Soc.* **1988**, *110*, 7870–7872.
(23) Billeter, M.; Basus, V. J.; Kuntz, I. D. *J. Magn. Reson.* **1988**, *76*, 400–415.
(24) Cieslar, C.; Clore, G. M.; Gronenborn, A. M. *J. Magn. Reson.* **1988**, *80*, 119–127.
(25) Kraulis, P. J. *J. Magn. Reson.* **1989**, *84*, 627–633.
(26) Kleywegt, G. J.; Lamerichs, R. M. J. N.; Boelens, R.; Kaptein, R. *J. Magn. Reson.* **1989**, *85*, 186–197.
(27) Englander, S. W.; Wand, A. J. *Biochemistry* **1987**, *26*, 5953–5958.